FEMS Microbiology Ecology, 2026, **102**(11), fiag123
https://doi.org/10.1093/femsec/fiag123
Published: 30 October 2026
Research article

Plasmid–plasmid interactions reshape extracellular vesicle cargo and antimicrobial resistance gene transfer potential

Faina Tskhay[1,‡], Haining Huang[2,‡], Robin Starke[1], Magali de la Cruz Barron[1], M. Pilar Garcillán-Barcia[3], Thomas U. Berendonk[1], Anja Worrich[2,4,*], Uli Klümper[1,*]

[1]Institute of Hydrobiology, Technische Universität Dresden, 01062 Dresden, Germany
[2]Department of Applied Microbial Ecology, Helmholtz Centre for Environmental Research – UFZ GmbH, 04318 Leipzig, Germany
[3]Instituto de Biomedicina y Biotecnología de Cantabria (IBBTEC), Consejo Superior de Investigaciones Científicas - Universidad de Cantabria. Santander, 39011 Santander, Spain
[4]Institute of Biotechnology, Faculty of Environment and Natural Science, Brandenburg University of Technology Cottbus-Senftenberg, 01968 Senftenberg, Germany
*Corresponding authors. Uli Klümper, TU Dresden, Institute of Hydrobiology, 01062 Dresden, Zellescher Weg 40, Germany. E-mail: uli.kluemper@tu-dresden.de; Anja Worrich, BTU Cottbus-Senftenberg, Institute of Biotechnology, 01968 Senftenberg, Universitätsplatz 1, Germany. E-mail: worrich@b-tu.de
‡These authors contributed equally. Order of authors was decided based on contribution to the writing of the initial draft.
Editor: Kornelia Smalla

Abstract

Plasmids are major drivers of bacterial horizontal gene transfer, including transfer of antimicrobial resistance. Plasmid dissemination extends beyond conjugation to include extracellular vesicle (EV)-mediated transport. Although bacterial EVs can carry plasmid DNA, mechanisms governing which plasmids are incorporated into EVs remain poorly understood. Here, we tested whether principles of conjugative plasmid transfer, including effects of plasmid mobility type and plasmid–plasmid interactions, extend to EV-mediated export. Using model conjugative (pKJK5) and mobilizable (RSF1010) resistance plasmids in two independent hosts, we quantified plasmid incorporation into EVs under single- and dual-plasmid conditions. Despite its lower intracellular copy number, the conjugative pKJK5 was preferentially incorporated into EVs, exceeding RSF1010 by 10- to 23-fold under single-plasmid carriage. Under co-residence, this pattern reversed: RSF1010 enrichment increased by 13- to 37-fold, whereas pKJK5 incorporation decreased by 2- to 7-fold, strongly deviating from stochastic expectations based on intracellular abundance, with effects conserved across hosts. This indicates that mobilizable plasmids exploit conjugative transfer machinery to access membrane-associated sites of preferential EV formation, thereby increasing their likelihood of EV incorporation. This demonstrates that EV cargo composition is not stochastic but is actively reshaped by plasmid-specific properties and plasmid–plasmid interactions, revealing a previously unrecognized mechanism influencing gene transfer in microbial communities.

Keywords extracellular vesicles, plasmid-plasmid interactions, vesicle cargo, mobilizable plasmids, gene transfer potential

Introduction

Bacterial extracellular vesicles (EVs) are membrane-derived, spherical nanoparticles with a size range of 20–300 nm that are released from the cell envelope through processes such as membrane blebbing (Orench-Rivera and Kuehn 2016, Toyofuku et al. 2019, Rima et al. 2025). Once considered mostly involved in bacterial waste disposal, EVs are now recognized as active contributors to bacterial survival and adaptation (Schwechheimer and Kuehn 2015, Turnbull et al. 2016, Toyofuku et al. 2023). The versatility of EVs is linked to their ability to encapsulate, transport, and release diverse cargo molecules to mediate intercellular communication, facilitate pathogenicity, deliver bioactive compounds, or protect bacterial cells against antibiotics (Fulsundar et al. 2014, Schwechheimer and Kuehn 2015, Toyofuku et al. 2023, De Langhe et al. 2024). Beyond the delivery of proteins and metabolites, EVs can also encapsulate and transfer genetic material, such as free nucleic acids and plasmids (Fulsundar et al. 2014, Tran and Boedicker 2017, Dell'Annunziata et al. 2021, Toyofuku et al. 2023, Zhang et al. 2025). These properties position EVs as a potential fourth mechanism of horizontal gene transfer (HGT) (Guerrero-Mandujano et al. 2017, Tran and Boedicker 2017, Brito 2021, Castañeda-Barba et al. 2024, Wen and Herman 2024, Garcillán-Barcia et al. 2025, Takano et al. 2025).

Received: 17 July 2026. **Revised:** 21 September 2026. **Accepted:** 27 October 2026
© The Author(s) 2026. Published by Oxford University Press on behalf of FEMS. This is an Open Access article distributed under the terms of the Creative Commons Attribution-NonCommercial License (https://creativecommons.org/licenses/by-nc/4.0/), which permits non-commercial re-use, distribution, and reproduction in any medium, provided the original work is properly cited. For commercial re-use, please contact reprints@oup.com for reprints and translation rights for reprints. All other permissions can be obtained through our RightsLink service via the Permissions link on the article page on our site-for further information please contact journals.permissions@oup.com

In bacteria, HGT is mediated by three "classical" mechanisms: conjugation, transformation, and transduction (Lorenz and Wackernagel 1994, Brito 2021, Arnold et al. 2022). However, unlike these conventional HGT mechanisms, EV-mediated transfer does not require cell contact, as in conjugation, nor is it limited by host specificity, as in transduction, or recipient competence, as in transformation (Thomas and Nielsen 2005, Guerrero-Mandujano et al. 2017, Tran and Boedicker 2017). In addition, vesicular encapsulation protects the genetic cargo from endonuclease degradation, thereby enabling long-distance and even inter-species transfer of genetic material (Fulsundar et al. 2014, Tran and Boedicker 2017). Given the central role of HGT in the spread of antimicrobial resistance (AMR) and virulence determinants within bacterial communities, additional mechanisms of HGT warrant further investigation (Burmeister 2015, Wintersdorff von et al. 2016, Haudiquet et al. 2022). Successful encapsulation and transfer of mobile and chromosomal genetic elements through bacterial EVs have already been reported in numerous studies (Fulsundar et al. 2014, Tran and Boedicker 2017, Biller et al. 2025, Takano et al. 2025). For example, EV-mediated transfer of β-lactamase-encoding plasmids in *Acinetobacter baylyi* resulted in the acquisition of ampicillin resistance by the recipient bacteria (Fulsundar et al. 2014).

Within the context of EV-mediated HGT, selective incorporation of specific gene clusters and genetic elements into EVs has been reported, suggesting that EV cargo is not randomly assembled (Biller et al. 2025, Takano et al. 2025). For example, selective packaging of plasmids, key vehicles of HGT in bacterial communities (Norman et al. 2009, Ares-Arroyo et al. 2024), into EVs could majorly affect how efficiently plasmid-encoded genes, such as ARGs, disseminate. The efficiency of plasmid packaging into EVs has previously been linked to plasmid-specific properties such as size, origin of replication, and intracellular copy number. Comparative studies have shown that high-copy-number plasmids are more frequently detected in vesicles than low-copy-number plasmids, suggesting that intracellular abundance contributes to packaging rates (Tran and Boedicker 2017, 2019). However, these observations are largely based on bacterial strains harboring a single plasmid.

In addition to intracellular abundance, the spatial organization of plasmids within the cell may influence their incorporation into EVs. Conjugative plasmids encode mobility (MOB) functions and membrane-associated mating pair formation (MPF) complexes required for their autonomous transfer between bacteria (Smillie et al. 2010, Garcillán-Barcia et al. 2025). These systems include type IV secretion machinery and coupling proteins that recruit plasmid DNA to the membrane-associated transfer complex, positioning it in proximity to the cell envelope (Llosa et al. 2003, Tato et al. 2005). In contrast, mobilizable plasmids encode only the MOB functions but lack the MPF complex and therefore depend on exploiting conjugative plasmids' MPF complexes for transfer (Haudiquet et al. 2022, Ares-Arroyo et al. 2024, Garcillán-Barcia et al. 2025). As a result, mobilizable plasmids are not inherently associated with membrane-bound transfer systems. Given that EVs originate from the cell envelope (Schwechheimer and Kuehn 2015, Roier et al. 2016, Toyofuku et al. 2019, 2023), these differences in membrane association may influence plasmid incorporation into EVs. However, existing observations are largely based on single plasmid systems and do not address how such relationships operate in more complex intracellular contexts.

In natural microbial communities, bacteria frequently carry multiple plasmids, and interactions between coexisting plasmids are common (Dionisio et al. 2019, Haudiquet et al. 2022, Ares-Arroyo et al. 2024, Garcillán-Barcia et al. 2025). Such interactions are well described for conjugative transfer, where mobilizable plasmids exploit conjugative machinery and can efficiently compete for access to type IV coupling proteins and membrane-associated transfer complexes (Smillie et al. 2010). These dynamics demonstrate that plasmid transfer is not solely determined by plasmid abundance or intrinsic properties, but also by interactions that affect access to membrane-associated systems. Whether plasmid–plasmid interactions between conjugative and mobilizable plasmids extend beyond conjugation to influence EV-mediated gene export remains unknown. Addressing this question is essential for understanding how EV cargo composition is determined under conditions that more closely reflect natural plasmid co-residence.

Taking into account the association of conjugative plasmids with the membrane and the high occurrence of plasmid interactions, which may influence incorporation of plasmids into EVs, we formulated two hypotheses: First, conjugative plasmids may be preferentially incorporated into EVs compared to mobilizable plasmids under single-plasmid conditions. Second, plasmid co-residence alters plasmid incorporation into EVs, consistent with reshaping access to and competition for positioning at membrane-associated transfer systems.

To test these hypotheses, we investigated the incorporation of a model conjugative low-copy-number plasmid (pKJK5) and a model mobilizable multicopy plasmid (RSF1010) into bacterial EV cargo across single- and dual-plasmid carriage states. We find that plasmid type and co-residence jointly shape EV cargo composition. While conjugative plasmids are preferentially incorporated into EVs in isolation, this pattern is altered under co-residence, where the mobilizable plasmid becomes enriched, and the conjugative plasmid is relatively depleted. This shift is consistent across different bacterial hosts, indicating that plasmid-plasmid interactions reshape EV-mediated gene export and represent a key determinant of EV cargo composition as well as a previously underappreciated layer of control in HGT.

Materials and methods

Bacterial strains

To test how plasmid type and plasmid co-residence influence incorporation into extracellular vesicles, we used two Gram-negative host backgrounds, *Escherichia coli* and *Pseudomonas putida*, and two model plasmids with distinct transfer strategies: the conjugative IncP-1 plasmid pKJK5 (Bahl et al. 2007) with a size of 57 419 base pairs and the 11 720 base pair, mobilizable IncQ plasmid RSF1010 (Meyer 2009), both carrying a GFP cassette (Klümper et al. 2014, 2015).

For each host, four strain types were required to address the hypotheses: a plasmid-free strain, strains carrying either pKJK5 or RSF1010 individually, and a strain carrying both plasmids. All strains were derived from *E. coli* K12::*lacI*^{q}-pLpp-*mCherry*-Km^{R} and *P. putida* KT2440::*lacI*^{q}-pLpp-*mCherry*-Km^{R} chromosomal backgrounds, as in these strains GFP expression is repressed and thus not a significant cost factor. The plasmid-free

and single-plasmid strains were already available from previous studies (Klümper et al. 2014, 2015). Therefore, to complete the set, we constructed strains carrying both plasmids in each host background.

To generate *E. coli* and *P. putida* strains carrying both plasmids, liquid mating was performed between the *E. coli* MG1655 carrying the RSF1010 plasmid that confers resistance to streptomycin and *P. putida* KT2440 carrying the pKJK5 plasmid that confers tetracycline resistance (Klümper et al. 2015). Overnight cultures of these strains were adjusted to $OD_{600} = 0.5$, mixed in a 1 : 1 ratio, and incubated overnight in Luria–Bertani (LB) medium (Merck KGaA, Darmstadt, Germany) at 120 r/m and 30°C. Successful acquisition of both plasmids was confirmed by plating 100 μl of the resulting mixed culture on selective media: Chromocult coliform agar for *E. coli* and Pseudomonas isolation agar (both Merck KGaA) for *P. putida,* supplemented with both antibiotics, streptomycin (100 μg/ml) and tetracycline (10 μg/ml). Together, these strains provided the full set of plasmid configurations required to test the hypotheses across both host backgrounds (Table 1).

EV isolation from liquid cultures

EVs from each of the 8 strains (2 species × 4 plasmid configurations) were isolated from liquid bacterial cultures following a previously reported extraction protocol (Manning and Kuehn 2011) with minor modifications. Briefly, each strain was first grown overnight on LB agar plates containing antibiotics corresponding to plasmid-encoded resistance markers. A single colony was inoculated into 1 L of LB medium and incubated at 37°C with shaking at 120 r/m until the late exponential growth phase ($OD_{600} = 1.0$) was reached. Cultures were centrifuged at 10 000 × *g* for 30 min to remove bacterial cells, and the supernatant was sequentially filtered through 0.45 μm and 0.22 μm filters (GVS North America, USA). The filtrates were concentrated using a 100 kDa cutoff tangential flow filtration system (Vivaflow 200, Sartorius, Germany). To ensure complete removal of bacteria, the concentrates were additionally filtered through a 0.22 μm cellulose membrane filter (Merck Millipore, Cork, Ireland). EVs were pelleted by ultracentrifugation of the concentrate at 100 000 × *g* for 2 h at 4°C using a SW32 Ti rotor (Beckman Coulter, USA), and resuspended in 200 μl PBS buffer. EV preparations were obtained from three independent biological replicates per condition (n = 3). To ensure that DNA detected in subsequent analyses was exclusively associated with EVs, samples were treated with 2 U of Turbo DNase (Invitrogen, USA) for 30 min at 37 °C. DNase was subsequently inactivated by heat treatment at 75°C for 15 min (Zhu et al. 2022). Genomic DNA and plasmid DNA extracted from *E. coli* carrying the pKJK5 plasmid served as positive controls to confirm the effectiveness of the DNase treatment, and DNA concentrations for both were reduced to below the limit of detection. DNA concentrations were subsequently quantified using a Qubit 3.0 fluorometer with the dsDNA HS Assay Kit (Invitrogen, Thermo Fisher Scientific).

Nanoparticle tracking analysis

Nanoparticle Tracking Analysis (NTA) was performed using a NanoSight LM10 instrument equipped with a 642 nm laser and a CCD camera (NanoSight Ltd., UK) to quantify the isolated EVs. Prior to sample analysis, instrument performance and focus were verified using 100 nm polystyrene latex standard beads (Malvern Panalytical). Samples were diluted in filtered 1× PBS (0.22 μm membrane) to adjust particle concentrations to the optimal measurement range of 1×10^7–1×10^8 particles/ml, and injected into the sample chamber with a sterile syringe. All measurements were conducted at a controlled temperature of 22°C. For each sample, a single 60 s video was captured. To minimize carryover between measurements, the sample chamber was flushed with ultrapure water prior to each injection. Data acquisition and processing were performed using NTA software version 2.0. All videos were analyzed using the following uniform settings: camera gain 1, detection threshold 12, blur size 3 × 3, minimum expected particle size 50 nm, and minimum track length 10. EV concentration (particles/ml) and size distribution were calculated from each video. These values were used to determine EV production per bacterial cell and plasmid copies per EV.

Duplex droplet digital PCR of EV fractions for plasmid quantification

Duplex droplet digital polymerase chain reaction (ddPCR) was performed to simultaneously detect and quantify the two plasmid targets (pKJK5::*gfp* and RSF1010::*gfp*) in extracted EVs. ddPCR enables absolute quantification based on a most-probable-number approach and does not require external calibration standards (Hindson et al. 2011). ddPCR was carried out using the QX200 Droplet Digital PCR System (Bio-Rad, Hercules, CA, USA). Each 20 μl of reaction mix contained 10 μl of ddPCR Supermix for Probes (No dUTP, Bio-Rad), two primer pairs targeting a 179 bp region in the *traJ* gene of the pKJK5 plasmid and a 169 bp region in the *aph(3′)-IIb* gene of the RSF1010 plasmid (final concentration of each primer 900 nM) and respective probes for pKJK5 labelled with a HEX fluorescence reporter and for RSF1010 labelled with a FAM reporter (final concentration 250 nM each) (Table 1). The selected target regions were chosen to enable simultaneous detection of both plasmid targets under the same ddPCR conditions due to their similar primer annealing temperatures. The specificity of the primer pairs was tested using RSF1010 plasmid-derived DNA as negative control for the primers targeting pKJK5 plasmid and pKJK5 plasmid-derived DNA as negative control for the primers targeting RSF1010 plasmid. In addition, the specificity against the chromosomal DNA of the respective *E. coli* and *P. putida* strains were confirmed by no amplification during PCR. These controls confirmed the specificity of each primer pair for each respective plasmid region. However, detection of these targeted regions does not demonstrate incorporation of complete plasmids into vesicles. EV extracts were diluted 1 : 10 in nuclease-free water, and 5 μl of the diluted EV suspension was used as a template. QX200™ Droplet Generator and Droplet Generation Oil for Probes (both Bio-Rad) were used for droplet generation. The PCR amplification was performed in a 96-well plate (Bio-Rad, Hercules, CA, USA) on a C1000 Touch Thermocycler (Bio-Rad, Hercules, CA, USA), under the following cycling conditions: 95°C for 10 min enzyme activation, 40 cycles of 94°C for 30 sec denaturation, 60°C for 1 min annealing, followed by a final hold at 98°C for 10 min. The ramp rate was set at 2°C/s. After amplification, the droplets were read using the QX200 Droplet Reader (Bio-Rad, Hercules, CA, USA). The data was analyzed using QuantaSoft software (Bio-Rad). This approach enabled absolute quantification of pKJK5 and RSF1010 copy numbers, which were subsequently used to calculate plasmid copies

Table 1 List of strains, plasmids, and primers used in this study.

Species/ Strain	Plasmid	Plasmid type	Plasmid carriage	Reference
Escherichia coli MG1655	–	–	Plasmid-free control	(Klümper et al. 2015)
E. coli MG1655	pKJK5::*gfp*,	IncP-1 (conjugative)	Single plasmid	(Meyer 2009)
E. coli MG1655	RSF1010::*gfp*	IncQ (mobilizable)	Single plasmid	(Klümper et al. 2015)
E. coli MG1655	pKJK5::*gfp* + RSF1010::*gfp*	IncP-1+ IncQ	Plasmid coexistence	This study
Pseudomonas putida KT2440	None	–	Plasmid-free control	(Klümper, et al. 2017)
P. putida KT2440	pKJK5::*gfp*	IncP-1	Single plasmid	(Meyer 2009)
P. putida KT2440	RSF1010::*gfp*	IncQ	Single plasmid	(Klümper et al. 2015)
P. putida KT2440	pKJK5::*gfp* + RSF1010::*gfp*	IncP-1 + IncQ	Plasmid coexistence	This study

Assay	Forward primer	Reverse primer	Probe	Target gene	Amplicon size	Reference
pKJK5::*gfp*	CTGTGATGCCCT TGATTTCG	AGGTTGGACGATGG AGAAAG	CCGGGAACACCGGC ACCCGC	*traJ*	179 bp	This study
RSF1010::*gfp*	TCTGTCTGGAGC GGATTTG	CGGTAAGAAGTCGG GATTG	CGCGAATGTTCGGA CGCGCCG	*aph(3′)-IIb*	169 bp	This study
16S rRNA	TCCTACGGGAGG CAGCAGT	ATTACCGCGGCTGC TGG	–	*16S rRNA* (V3 region)	195 bp	(Muyzer et al. 1993)

Km = Kanamycin, Tet = Tetracycline, Strep = Streptomycin.

per EV. All ddPCR reactions were performed in technical duplicates for each independent biological replicate (n = 3).

Extraction of bacterial genomic DNA

To quantify intracellular plasmid copy numbers per bacterial cell, total genomic DNA was extracted from strains carrying either single plasmids or both coexisting plasmids. Total genomic DNA was extracted using the DNeasy PowerSoil Kit (Qiagen, Hilden, Germany) according to the manufacturer's protocol, with modifications to sample preparation. Briefly, instead of 250 mg of solid sample, 2 ml of $OD_{600} = 1$ bacterial cultures grown under conditions identical to those used for EV extraction was centrifuged at 10 000 × g for 1 min, and the resulting pellet was used for subsequent DNA extraction. DNA concentrations were quantified using a NanoDrop 2000 (Thermo Fisher, Waltham, MA, USA), and quality was assessed based on the 260/280 nm absorbance ratio, which ranged between 1.8 and 2.0 for all samples. Extracted DNA was stored at –20°C until further analysis. Three independent biological replicates per condition were used for DNA extraction.

Droplet digital PCR of bacterial chromosomal marker DNA

Plasmid copy number per bacterial cell was quantified using duplex ddPCR as described for EV extracts. DNA samples were normalized to 2 ng/μl and diluted 1 : 500 in nuclease-free water to avoid droplet saturation. In addition, ddPCR using the EvaGreen Assay targeting the 16S rRNA gene was performed with total bacterial genomic DNA to quantify total cell numbers. Similarly, the 16S rRNA gene was also quantified in the EV suspension to obtain a plasmid-to-16S ratio. Each 20 μl reaction contained 10 μl of ddPCR EvaGreen Supermix (Bio-Rad), the 331F/518R primer pair targeting a 195 bp region of the 16S rRNA gene (final concentration 250 nM) (Table 1) (Muyzer et al. 1993), 5 μl of the diluted DNA or 5 μl of diluted EV suspension were used as template. Droplet generation, thermal cycling, droplet reading, and data analysis were performed as described above. This approach enabled calculation of intracellular plasmid copy numbers per bacterial cell by normalizing plasmid abundance to total cell counts using the known content of seven 16S rRNA gene copies/cell in *E. coli* (Johnson et al. 2019) and seven gene copies/cell in *P. putida* (Nelson et al. 2002).

Data processing, visualization, and calculation of EV plasmid incorporation

Data analysis was performed in RStudio v. 2026.01.0+392 (Posit team 2024), and the R package ggplot2 v.3.5.1(Wickham 2016) was used for data visualization. The analyzed variables included vesicle concentrations (vesicles per milliliter), vesicle production (vesicles per bacterial cell), plasmid copy numbers per vesicle, plasmid copy numbers per cell, and derived measures such as the fraction of intracellular plasmids incorporated into EVs and observed-to-expected plasmid ratios.

To estimate the fraction of the intracellular plasmid pool incorporated into EVs, total EV-associated plasmid copies were compared to total intracellular plasmid abundance in the cultures.

Since EVs were isolated from 1 l of bacterial culture and resuspended in 200 μl, we first scaled all vesicle concentrations to the original culture volume by multiplying vesicle concentration in the EV suspension by the resuspension volume (0.2 ml). The total plasmid copies associated with EVs were then calculated by multiplying plasmid copy number per vesicle by the total number of vesicles in 1 l of the original culture. The intracellular plasmid abundance was estimated by multiplying plasmid copy number per cell by the number of cells per milliliter and scaling this value to 1 l.

The total intracellular plasmid abundance was calculated as the product of the plasmid copy number per cell and the cell density (cells per milliliter) estimated from OD_{600} measurements. The fraction of plasmid in vesicles was thus calculated as:

$$\textit{Fraction of plasmids in vesicles} = \frac{\textit{Plasmid copy/Vesicle} * \textit{Vesicle concentration}/\text{mL} * 0.2\ \text{mL}}{\textit{Plasmid copy/Cell} * \textit{Cells}/\text{mL} * 1000\ \text{mL}}.$$

This fraction was then used to calculate expected plasmid copy numbers per vesicle under a stochastic packaging model, assuming proportional incorporation based on intracellular abundance:

$$\textit{Plasmid per Vesicle (expected)} = \frac{\textit{Plasmid copies/Cell} * \textit{Cell number} * \textit{Fraction of plasmids in vesicles}}{\textit{Vesicle number}}.$$

A linear model was fitted to log-transformed vesicle numbers to assess the effect of plasmid carriage on EV production. Plasmid carriage (no plasmid, single-plasmid, and dual-plasmid) was set as an explanatory variable. Similarly, a linear model was fitted to log-transformed intracellular plasmid copy numbers to assess the effects of host background, plasmid identity, and coexistence state, with these factors included as explanatory variables. The model included all main effects and their interactions. Effect sizes were estimated using partial eta squared (η^2). A t-test was used to determine if plasmid incorporation in the vesicles with coexisting plasmids deviates from the stochastic model assuming proportional packaging based on single-plasmid EV packaging and intracellular plasmid abundance. A one-sided Wilcoxon rank-sum test was applied to assess whether EV-associated plasmid-to-16S rRNA gene ratios are higher than intracellular ratios. Throughout, statistical significance was assumed for $P < 0.05$.

Results

Vesicle production is primarily determined by host background and not consistently influenced by plasmid carriage

We first assessed whether vesicle production differed between host backgrounds and plasmid carriage states. We thus quantified vesicle production of *E. coli* and *P. putida* strains carrying either: (i) no plasmids, (ii) pKJK5 or (iii) RSF1010 individually, or (iv) coexisting RSF1010 and pKJK5 plasmids. Using nanoparticle tracking analysis, we detected vesiculation in all tested strains (Fig. 1A).

To quantify the contribution of host and plasmid effects, we fitted a linear model on log-transformed vesicle production data, including host background, pKJK5 presence, and RSF1010 presence as factors. This analysis identified a significant effect of the host background on of vesicle production ($\eta^2 = 0.42$, $P < 0.0001$), with *E. coli* producing significantly more vesicles per cell (1.6–4.8 $\times 10^{-3}$) than *P. putida* (0.3–2.6 $\times 10^{-3}$). Plasmid carriage-related effects were variable and strongly host-dependent (Fig. 1A). While pKJK5 showed a moderate effect in *E. coli,* RSF1010 was associated with increased vesicle production in *P. putida*, as reflected by significant host–plasmid interaction terms ($\eta^2 = 0.25$, $P < 0.0001$). However, these effects were not consistent across hosts and did not represent a generalizable influence of plasmid carriage on vesicle production.

Together, these results indicate that host physiology accounts for a substantial proportion of the variation in vesicle production, whereas the effect of the RSF1010 plasmid on vesiculation level was host-dependent, the effect of the pKJK5 plasmid is relatively minor under the tested conditions. Therefore, the differences in vesicle production alone cannot fully explain differences in EV plasmid-cargo composition observed below, which motivated us to examine whether intracellular plasmid abundance could explain the observed differences.

Intracellular plasmid abundance is stable and defines expected packaging ratios

To establish the baseline intracellular plasmid abundance, we quantified plasmid copy number per cell for both plasmids in single-plasmid and coexisting conditions across both bacterial hosts. As expected, the multicopy plasmid RSF1010 was consistently more abundant than the low-copy-number plasmid pKJK5 across all conditions (Fig. 1B).

A linear model on log-transformed copy numbers, including host background, plasmid identity, and coexistence state, identified plasmid identity as the dominant determinant of intracellular abundance ($\eta^2 = 0.84$, partial $\eta^2 = 0.93$, $P < 0.0001$). In contrast, host background had a significant but small effect ($\eta^2 = 0.003$, partial $\eta^2 = 0.05$, $P < 0.05$). Coexistence alone did not significantly affect intracellular copy number overall ($\eta^2 = 0.03$, partial $\eta^2 = 0.34$, $P = 0.9$) but a significant interaction between host and coexistence was observed ($\eta^2 = 0.03$, partial $\eta^2 = 0.36$, $P < 0.01$), indicating coexistence effect on plasmid copy number was host-dependent. No significant other interaction terms were detected (all $P > 0.05$).

Consistent with this, in *E. coli*, pKJK5 copy number remained essentially unchanged between single-plasmid and coexisting conditions (1.03 $\pm$ 0.19 vs 1.02 $\pm$ 0.30 copies per cell), while RSF1010 showed only a minor increase (4.83 $\pm$ 1.65 vs 5.19 $\pm$ 0.89). In *P. putida*, pKJK5 decreased from 1.76 $\pm$ 0.72 to 0.69 $\pm$ 0.21 copies per cell under coexistence, whereas RSF1010 decreased more moderately from 6.70 $\pm$ 0.42 to 5.46 $\pm$ 1.50. Accordingly, the intracellular RSF1010 : pKJK5 ratio was $\sim$5 : 1 in *E. coli* under coexisting conditions. A corresponding $\sim$5 : 1 plasmid copy number ratio was observed when comparing plasmid copy numbers between the RSF1010-carrying and pKJK5-carrying *E. coli* strains. In *P. putida,* the RSF1010 : pKJK5 ratio increased from $\sim$3.8 : 1 between the *P. putida* strain carrying a single RSF1010 plasmid and the *P. putida* strain carrying a single pKJK5 plasmid to a 7.9 : 1 ratio observed under coexistence. Together, these results show that intracellular plasmid abundance is primarily defined by plasmid identity and does not show consistent shifts across hosts. The intracellular ratios of the two plasmids, therefore, provide the null expectation

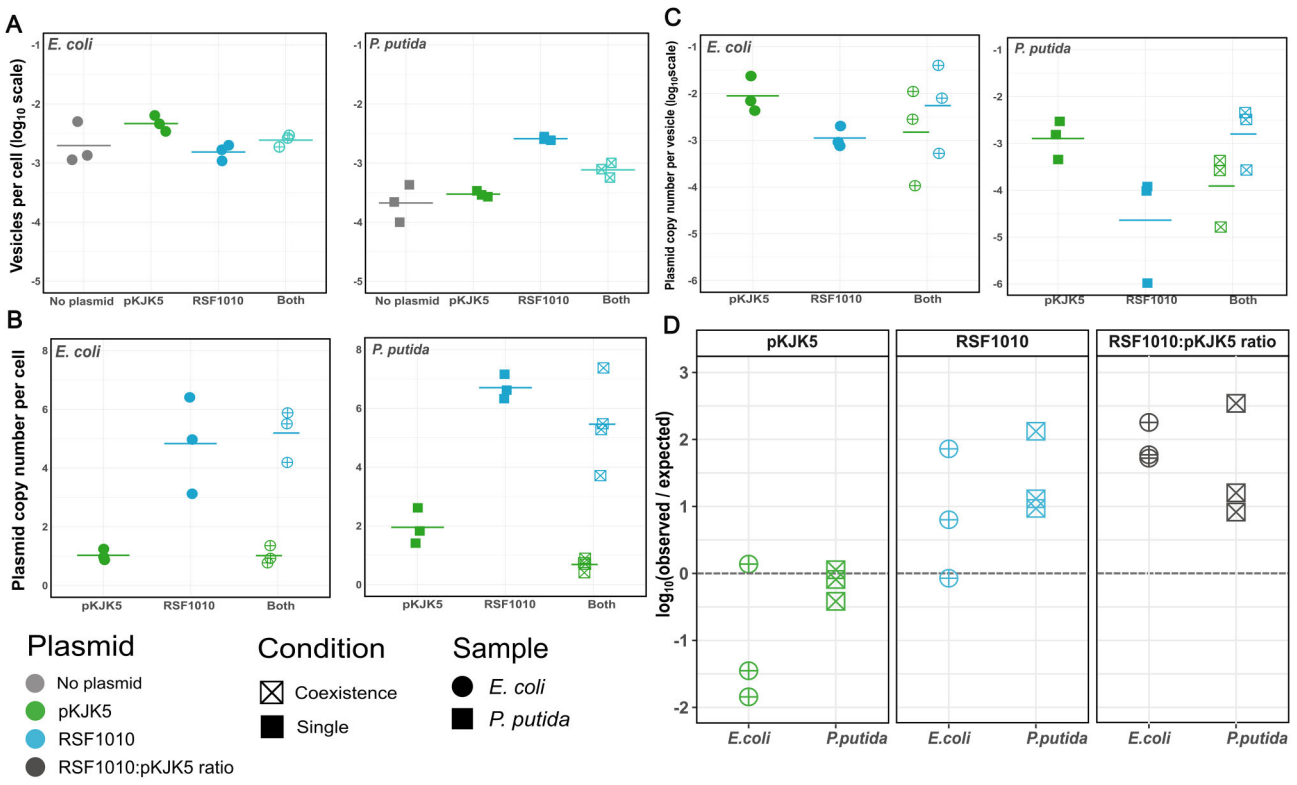


Figure 1 Effects of plasmid coexistence on vesicle production and plasmid incorporation into EVs produced by *E. coli* and *P. putida*. (A) Log_{10}-transformed number of EVs produced per cell by *E. coli* and *P. putida* strains with no plasmid, a single plasmid, and dual plasmid carriage. (B) Intracellular plasmid copy number per cell in strains harboring single or coexisting plasmids. (C) Log_{10}-transformed plasmid copy number per EV. (D) Log_{10} -transformed ratio of observed to expected EV-associated plasmid abundance. The dashed line indicates the stochastic expectation of plasmid incorporation into EVs (log_{10}(observed/expected) = 0). Expected values were derived from plasmid incorporation observed under single plasmid conditions and intracellular plasmid abundance observed under plasmid coexistence. Individual points represent three independent biological replicates (n = 3), with two technical replicates per biological replicate. For the intracellular RSF1010 ratio calculation in *P. putida* under plasmid coexistence, n = 4 independent measurements were used.

for stochastic EV packaging tested below assuming that plasmid packaging into EVs reflects their intracellular abundance.

Conjugative plasmids are preferentially incorporated into EVs in isolation

We next quantified the association of DNA originating from the plasmids with EVs under single plasmid conditions (Fig. 1C). Across both hosts, the conjugative plasmid pKJK5 was consistently enriched in EVs relative to the mobilizable plasmid RSF1010, despite its lower intracellular abundance and larger size.

In *E. coli,* pKJK5 target copy numbers reached $1.2 \pm 1 \times 10^{-2}$ copies per vesicle, ~10-fold higher than RSF1010 target copy numbers ($1.2 \pm 0.7 \times 10^{-3}$). In *P. putida*, this enrichment was even more pronounced, with pKJK5-target copy numbers exceeding those of RSF1010 by ~23-fold. Given the higher intracellular abundance of RSF1010, stochastic packaging would predict its dominance in EVs, with expected RSF1010 : pKJK5 ratios of ~5 : 1 in *E. coli* and 3.8 : 1 in *P. putida*. Instead, the observed ratios were reversed, with DNA originating from pKJK5 significantly dominating EV cargo above stochastic expectation in both hosts (t-test, $P < 0.001$).

Thus, under single-plasmid conditions, EV-associated plasmid composition does not reflect intracellular abundance but instead shows a consistent enrichment of the conjugative plasmid across host backgrounds. These findings support the hypothesis that plasmid-specific properties, such as membrane association potentially linked to conjugative transfer machinery, promote preferential incorporation of conjugative plasmids into EVs.

However, natural bacterial systems frequently involve co-resident plasmids, where interactions between plasmids can alter access to membrane-associated transfer machinery. We therefore next tested whether such interactions reshape plasmid incorporation into EVs beyond patterns observed under single-plasmid conditions.

Plasmid co-residence reverses EV cargo composition and deviates from stochastic expectations

To test whether plasmid–plasmid interactions alter EV cargo composition, we quantified association of plasmid-derived DNA with EVs under coexisting conditions and compared observed values to expectations based on intracellular plasmid abundance. Under plasmid co-residence, EV cargo composition shifted markedly in both hosts. In contrast to single-plasmid conditions, copy numbers of the RSF1010 target became dominant in EVs, exceeding

those of pKJK5 by approximately four-fold in *E. coli* and 11-fold in *P. putida* (Fig. 1C).

In absolute terms, the RSF1010 target copy number increased from $1.2 \pm 0.7 \times 10^{-3}$ to $1.6 \pm 1 \times 10^{-2}$ copies per vesicle in *E. coli*, corresponding to an ∼13-fold enrichment under coexistence. In *P. putida*, the RSF1010 target copy number increased from $7.3 \pm 6 \times 10^{-5}$ to $2.7 \pm 2 \times 10^{-3}$ copies per vesicle, corresponding to an ∼37-fold enrichment. In contrast, copy numbers of the pKJK5 target decreased from $1.2 \pm 1 \times 10^{-2}$ to $5 \pm 5 \times 10^{-3}$ copies per vesicle in *E. coli* (∼2.4-fold reduction), and from $1.7 \pm 1.2 \times 10^{-3}$ to $2.4 \pm 2 \times 10^{-4}$ in *P. putida* (approximately seven-fold reduction).

Species-specific analyses showed consistent directional shifts in EV-associated plasmid ratios. Based on the intracellular plasmid abundance and single-plasmid EV packaging patterns above, expected RSF1010 : pKJK5 ratios would have remained ∼0.10 in *E. coli* and 0.04 in *P. putida*. Instead, under coexistence, the observed ratios increased to ∼4 and 11, respectively.

Comparison to stochastic expectations revealed that the RSF1010 target was significantly enriched in EVs relative to predicted values across both species (one-sample t-test, $P < 0.01$), whereas the pKJK5 target showed a consistent reduction ($P = 0.14$). Consequently, the EV-associated RSF1010 : pKJK5 ratio significantly deviated from the expected ratio ($P < 0.001$) (Fig. 1D). Under a stochastic packaging model, EV-associated plasmid composition would be expected to reflect intracellular abundance and the packaging bias observed under single-plasmid conditions. Instead, plasmid co-residence shifted EV cargo toward dominance of the mobilizable plasmid.

Conjugative pKJK5 is enriched relative to chromosomal DNA in EVs

To further characterize the association of plasmid DNA with extracellular vesicles, we compared the relative abundance of the plasmid-derived DNA to a chromosomal marker (V3 region of the *16S rRNA* gene) between EV and intracellular fractions (Fig. 2A and B). Across all conditions containing pKJK5, the plasmid-to-16S ratio was significantly higher in EV fractions than in the corresponding cellular DNA extracts (one-sided Wilcoxon test, $P = 0.03$), indicating preferential enrichment of the conjugative plasmid relative to the 16S rRNA marker during EV association (Fig. 2C). In contrast, the plasmid-to-16S ratio of the mobilizable plasmid RSF1010 did not differ significantly between EVs and cells (one-sided Wilcoxon test, $P = 0.23$). These findings demonstrate that pKJK5-derived DNA is enriched relative to the chromosomal marker within EV fractions, supporting selective plasmid association with extracellular vesicles rather than simple proportional release of cellular DNA, when conjugative plasmids with membrane-associated components of their transfer system are present.

Together, these results demonstrate that plasmid incorporation into EVs is non-random and is actively reshaped by plasmid–plasmid interactions, supporting the second hypothesis. This interaction-driven restructuring of EV cargo was conserved across both hosts, despite big differences in vesicle production and host-specific plasmid effects. This decoupling demonstrates that EV cargo composition is not governed by vesicle production dynamics, but instead by selective processes linked to plasmid-specific properties and their interactions. Thus, plasmid–plasmid interactions define EV-mediated gene transfer outcomes independently of vesicle abundance. However, it is worth stressing that these results are limited by the two bacterial strains and the combination of only two plasmids tested here. Studies involving other bacterial hosts carrying other combinations of mobilizable and conjugative plasmids are needed to further confirm whether these patterns reflect a broader trend.

Discussion

In this study, we investigated whether principles governing plasmid transfer, including plasmid mobility type and plasmid–plasmid interactions (Dionisio et al. 2019, Ares-Arroyo et al. 2024, Garcillán-Barcia et al. 2025), extend beyond conjugation to influence their incorporation into EVs. Specifically, we tested whether conjugative and mobilizable plasmids differ in their propensity for EV incorporation, and whether plasmid co-residence alters this pattern through interactions between coexisting plasmids. Whereas both plasmids were detected in EVs, the EV fraction with pKJK5 as cargo dominated over that with RSF1010 in strains carrying individual plasmids. In contrast, under coexistence, this relationship was reversed, with RSF1010 enriched and pKJK5 depleted in EV cargo. These effects were consistent across both bacterial hosts. Together, these findings suggest that plasmid incorporation into EVs is not solely determined by intracellular abundance but is influenced by plasmid-specific properties and their interactions, extending plasmid transfer dynamics beyond classical conjugation.

The preferential incorporation of pKJK5 under single-plasmid conditions diverges from its lower intracellular abundance relative to RSF1010, challenging the assumption that EV packaging is driven by plasmid copy number alone (Tran and Boedicker 2017, 2019). A similar pattern of overall EV-associated pKJK5 prevalence was observed when plasmid copies were normalized to the 16S rRNA gene, while the ratio of RSF1010 copies per 16S rRNA gene did not differ between EV-associated and intracellular fractions. A plausible explanation is the spatial localization of plasmids within the bacterial cell. Similar to other conjugative plasmids, pKJK5 encodes a type IV secretion system (T4SS) that enables its autonomous transfer between bacteria (Smillie et al. 2010, Garcillán-Barcia et al. 2025). Autonomous transfer requires assembly of the T4SS, including coupling proteins and associated components that localize the plasmid-relaxosome complex at the cell membrane (Segura et al. 2014, Carranza et al. 2021), thereby positioning plasmid DNA in proximity to the cell envelope. In contrast, mobilizable plasmids such as RSF1010 lack the MPF system (Meyer et al. 1982, Meyer 2009) and therefore do not encode a dedicated transfer apparatus for organized membrane localization. Although mobilizable plasmids can associate with the membrane, for example via the MobB protein of RSF1010 (Parker and Meyer 2007), this association is likely less structured than that of conjugative plasmids. As EVs originate from the bacterial membrane, the incorporation of the components that are more consistently localized at the membrane is expected to be more efficient, which could favour conjugative over mobilizable plasmids.

Differences in plasmid replication biology may also contribute to EV incorporation. pKJK5 possesses a TrfA-dependent theta-replication system, whereas RSF1010 uses RepA-, RepB′- and RepC-dependent strand-displacement replication, which gener-

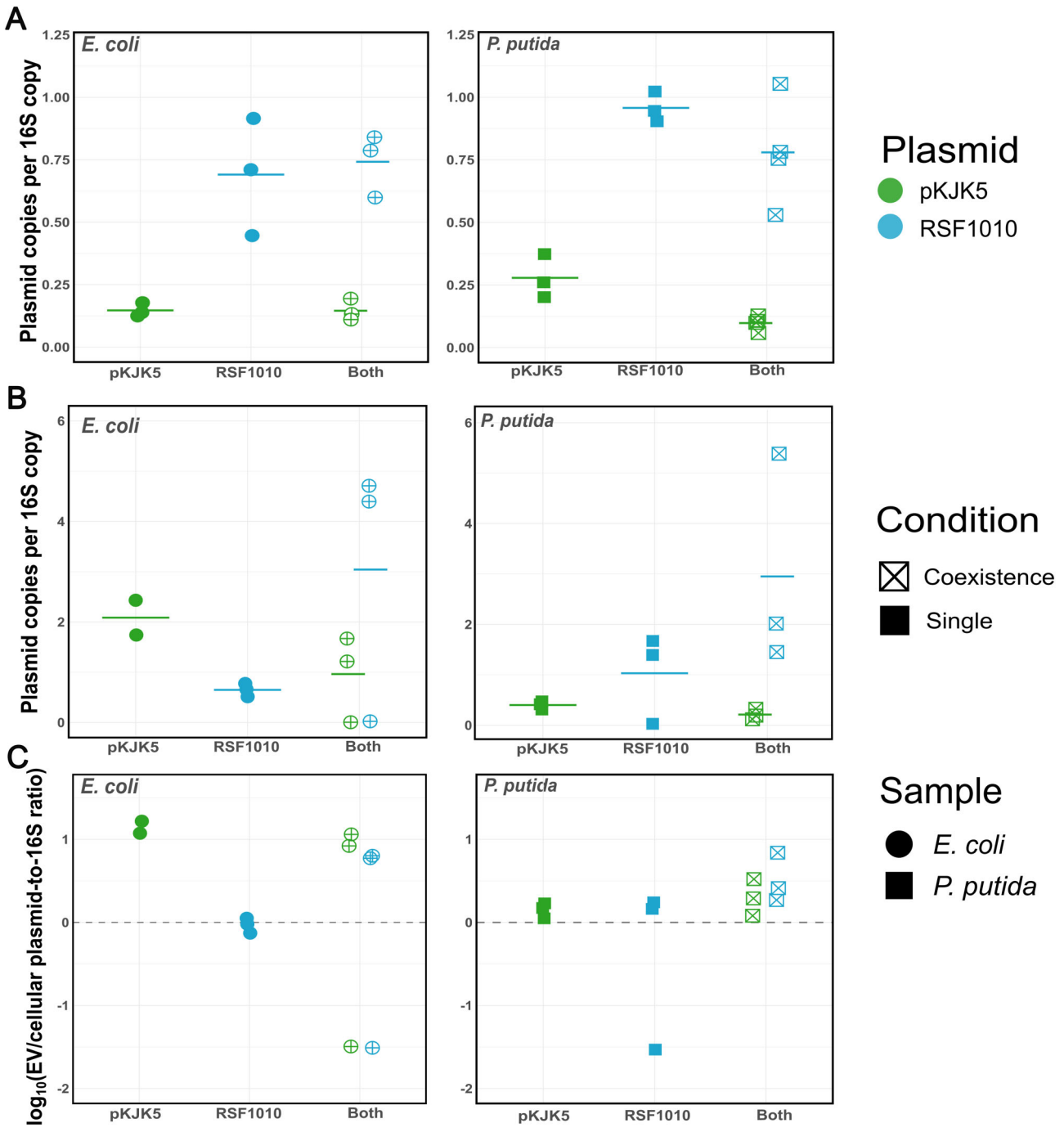


Figure 2 Plasmid-to-16S rRNA gene ratios in *E. coli* and *P. putida*. (A) Intracellular ratios of pKJK5 and RSF1010 plasmid copies to the 16S rRNA gene in strains harboring single or coexisting plasmids. (B) EV-associated ratio of pKJK5 and RSF1010 plasmid copies to the 16S rRNA gene copies. (C) Log10-transformed ratios of EV-associated to intracellular plasmid-to-16S rRNA gene ratios. The dashed line at 0 indicates equal EV-associated and intracellular plasmid-to-16S rRNA ratios. Individual points represent three independent biological replicates (n = 3), with two technical replicates per biological replicate. For the intracellular RSF1010 ratio calculation in *P. putida* under plasmid coexistence, n = 4 independent measurements were used.

ates abundant single-stranded DNA intermediates (Bahl et al. 2007, Meyer 2009). These differences could affect plasmid topology, protein association and subcellular localization, all of which may influence the accessibility of plasmid molecules for EV packaging. Consistent with this possibility, replication origin has previously been shown to affect plasmid loading into bacterial EVs beyond its influence on intracellular copy number (Tran and Boedicker 2019). Such intrinsic differences may contribute to the baseline packaging efficiencies of pKJK5 and RSF1010. However, because their replication mechanisms remain unchanged between the single- and dual-plasmid conditions, they cannot alone explain the co-residence-dependent reversal in plasmid incorporation. Co-residence could nevertheless alter the abundance or localization of replication intermediates, potentially contributing to cargo redistribution alongside recruitment of RSF1010 by the pKJK5 conjugative machinery.

An additional, but likely secondary, mechanism could involve local bacterial outer membrane disturbance (Nagakubo et al. 2020) associated with T4SS assembly and pilus formation (Collins et al. 2005), which has been proposed to promote vesiculation. However, in our data, plasmid carriage did not lead to consistent increases in EV production across hosts, indicating that plasmid-induced membrane perturbation is not a dominant driver of EV formation. Given that EV production is largely governed by host background and likely includes contributions from both membrane blebbing or cell lysis (Schwechheimer and Kuehn 2015, Turnbull et al. 2016, Toyofuku et al. 2023), the observed enrichment of pKJK5 relative to chromosomal material and the RSF1010 plasmid occurs despite this heterogeneous EV background. Importantly, the proposed mechanism of membrane proximity does not depend on a specific mode of EV biogenesis, as vesicles derived from either membrane blebbing or cell lysis are equally expected to selectively capture membrane-associated material (Toyofuku et al. 2023). Together, these observations support a model in which spatial proximity to membrane-associated transfer machinery, rather than EV production per se, contributes to the preferential incorporation of conjugative plasmids into EVs.

Plasmid co-residence can influence access to membrane-associated transfer machinery, as mobilizable plasmids exploit conjugative systems and coexisting plasmids can interfere with each other's transfer (Ares-Arroyo et al. 2024). In contrast to single-plasmid conditions, coexistence reversed EV cargo composition, suggesting that interactions between conjugative and mobilizable plasmids reshape access to sites of preferential EV cargo incorporation. In multi-plasmid conjugative systems, mobilizable plasmids are known to exploit the transfer machinery encoded by conjugative plasmids, and RSF1010 is a well-characterized example that is efficiently mobilized by IncP-1 plasmids such as pKJK5 (Haase et al. 1995, Meyer 2009, Klümper et al. 2014). This process relies on the affinity between the relaxosome of the mobilizable plasmid and the type IV coupling protein (T4CP) complex of the conjugative system, which determines access of RSF1010 to membrane-associated transfer sites and thereby its mobilization efficiency (Cabezón et al. 1997). Under coexistence, such interactions may lead to preferential recruitment of RSF1010 to these membrane-associated sites, increasing its proximity to the cell envelope and thereby its likelihood of incorporation into EVs. At the same time, this recruitment is expected to reduce the availability of T4CPs and associated transfer complexes for pKJK5 itself, probably resulting in its relative depletion from membrane-associated regions and consequently from EV cargo, as has been shown for other conjugative-mobilizable plasmid pairs (Ceccarelli et al. 2008, Carraro et al. 2017). Thus, competition for and preferential access to membrane-associated transfer machinery could potentially explain the enrichment of RSF1010 and the depletion of pKJK5 observed under plasmid coexistence. These findings suggest that interactions between mobilizable and conjugative plasmids may influence not only direct gene transfer through conjugation but also which genetic elements enter the extracellular gene pool through EVs.

Despite pronounced differences in EV production observed between hosts, the direction of plasmid packaging dynamics was conserved. This indicates that host background primarily modulates EV abundance and effect size, while plasmid–plasmid interactions determine cargo composition. Host physiology may nonetheless influence the ecological relevance of this mechanism. In *P. putida*, EV production is more strongly associated with stress responses and membrane instability, whereas in *E. coli*, vesiculation occurs at a higher basal level (McBroom et al. 2006, Kulp et al. 2015, Bitzenhofer et al. 2024). Under stress conditions, which represent windows of bacterial adaptation where plasmid-encoded traits can provide strong selective advantages (Johnson and Nolan 2009, Coluzzi et al. 2022, Castañeda-Barba et al. 2024), increases in EV production may amplify the interaction-driven restructuring of plasmid cargo observed here, thereby contributing more substantially to extracellular gene flux. In complex natural microbial communities, where both stress exposure and multi-plasmid carriage are common, these dynamics may influence not only which plasmids are transferred, but also which host populations contribute to EV-mediated gene pools. Given that mobilizable plasmids are often overrepresented in natural microbial communities (Petersen et al. 2019, Ares-Arroyo et al. 2024, Fogarty et al. 2024, Tamayo-Leiva et al. 2024), which can be related to their smaller size, lower intrinsic costs, and ability to utilize conjugative plasmids for transfer (San Millan and MacLean 2017, Garcillán-Barcia et al. 2019, Coluzzi et al. 2022), the plasmid–plasmid interactions described here are likely widespread. Our results suggest that such interactions may extend beyond conjugation to shape the composition of extracellular genetic material, with potential consequences for the dissemination of AMR genes and other adaptive traits.

The above formulated results entail several limitations. First, we focused on a single pair of model plasmids, and different combinations of conjugative and mobilizable plasmids may exhibit distinct interaction dynamics and packaging behavior. Second, the detection of plasmid association with EV was based on a specific region of the plasmid DNA rather than using a complete plasmid molecule. Third, the experiments were conducted in two bacterial hosts under controlled laboratory conditions, and vesicle-mediated packaging patterns may differ in more complex microbial communities. Fourth, the proposed mechanism linking plasmid interactions to membrane-associated positioning and EV incorporation remains inferred rather than directly demonstrated. Future work should therefore expand to additional plasmid combinations and incompatibility groups, including different plasmid variants and targeted mutants with altered mobilization or coupling functions (Cabezón et al. 1997), to directly test the role of conjugation machinery in mediating plasmid recruitment into vesicles. Direct visualization of plasmid localization relative to the cell envelope, for example, using fluorescence-based approaches (Yao et al. 2007) would provide critical evidence for spatial positioning as the suggested driver of EV incorporation. Using primer pairs targeting additional regions of each plasmid or multiplex ddPCR targeting multiple regions of plasmid DNA would also help determine whether complete plasmid molecule or rather plasmid fragments are incorporated into EV. Beyond controlled systems, extending these analyses to more complex microbial communities will be essential to determine whether the interaction-driven restructuring of EV cargo observed here persists under environmentally relevant conditions. Finally, assessing the functional consequences of EV-mediated plasmid transfer, including uptake and establishment in recipient bacteria and their rates relative to established HGT mechanisms, will be critical to evaluate its ecological and evolutionary significance.

In summary, our results suggest that plasmid incorporation into extracellular vesicles is not fully explained by stochastic pro-

cesses or intracellular abundance alone, but may be shaped by plasmid-specific properties and their interactions. Conjugative plasmids are preferentially incorporated under single-plasmid conditions, while plasmid co-residence reverses this pattern through interaction-driven restructuring of access to membrane-associated transfer machinery. These findings extend the role of plasmid–plasmid interactions beyond conjugation and identify them as a key determinant of extracellular gene transfer. Given the ubiquity of vesiculation and multi-plasmid carriage in microbial communities, this mechanism may represent a previously unrecognized route by which plasmid interactions shape the dissemination of antibiotic resistance and other adaptive traits.

Acknowledgements

The authors thank Christiane Zschornack, Melanie Tannert, and Steffen Kunze for technical support in the laboratory.

Author contributions

Faina Tskhay (Conceptualization, Data curation, Formal Analysis, Investigation, Methodology, Validation, Visualization, Writing—original draft, Writing—review & editing), Haining Huang (Conceptualization, Formal Analysis, Funding acquisition, Investigation, Methodology, Visualization, Writing—review & editing), Robin Starke (Data curation, Formal Analysis, Methodology, Writing—review & editing), Magali de la Cruz Barron (Methodology, Writing—review & editing), M. Pilar Garcillán-Barcia (Writing—review & editing), Thomas Berendonk (Conceptualization, Funding acquisition, Project administration, Resources, Supervision, Visualization, Writing—review & editing), Anja Worrich (Conceptualization, Funding acquisition, Project administration, Resources, Supervision, Writing—review & editing), and Uli Klümper (Conceptualization, Data curation, Funding acquisition, Methodology, Project administration, Resources, Supervision, Visualization, Writing—original draft, Writing—review & editing)

Conflict of interest

The authors declare no conflicts of interests.

Funding

This work was supported by the JPIAMR TEXAS, the JPIAMR SEARCHER, and the Explore-AMR project funded by the German Bundesministerium für Forschung, Technologie & Raumfahrt under grant numbers 01KI2401, 01KI2404A & 01DO2200. F.T., R.S., and T.U.B. received support from the DFG-funded TARGIM project (512064678). U.K. and F.T were supported through the ONE-BRIDGE project funded by the EU4Health Program (EU4H) under project number 101233407 and the MOBSTER project funded by the DAAD (Project ID: 57751373). H.H. acknowledges the support of the China Scholarship Council program (202304910040). A.W. was supported by the DFG Emmy Noether Program (530107960). M.P.G.B. was supported by the Spanish Ministry of Science and Innovation (Grant MCIN/AEI/10.13039/501100011033 PID2020-117923GB-I00). Responsibility for the information and views expressed in the manuscript lies entirely with the authors.

Data availability

The datasets supporting the conclusions of this article are included within the article and its additional files or available through the corresponding authors upon reasonable request.

References

Ares-Arroyo M, Coluzzi C, Moura de Sousa JA *et al.* Hijackers, hitchhikers, or co-drivers? The mysteries of mobilizable genetic elements. *PLoS Biol* 2024;**22**:e3002796. https://doi.org/10.1371/journal.pbio.3002796.

Arnold BJ, Huang IT, Hanage WP. Horizontal gene transfer and adaptive evolution in bacteria. *Nat Rev Micro* 2022;**20**:206–18. https://doi.org/10.1038/s41579-021-00650-4.

Bahl MI, Hansen LH, Goesmann A *et al.* The multiple antibiotic resistance IncP-1 plasmid pKJK5 isolated from a soil environment is phylogenetically divergent from members of the previously established α, β and δ sub-groups. *Plasmid* 2007;**58**:31–43. https://doi.org/10.1016/j.plasmid.2006.11.007.

Biller SJ, Ryan MG, Li J *et al.* Distinct horizontal gene transfer potential of extracellular vesicles versus viral-like particles in marine habitats. *Nat Commun* 2025;**16**:2126. https://doi.org/10.1038/s41467-025-57276-w.

Bitzenhofer NL, Höfel C, Thies S *et al.* Exploring engineered vesiculation by Pseudomonas putida KT2440 for natural product biosynthesis. *Microb Biotechnol* 2024;**17**:e14312. https://doi.org/10.1111/1751-7915.14312.

Brito IL. Examining horizontal gene transfer in microbial communities. *Nat Rev Micro* 2021;**19**:442–53. https://doi.org/10.1038/s41579-021-00534-7.

Burmeister AR. Horizontal Gene Transfer. *EMPH* 2015;**2015**:193–4. https://doi.org/10.1093/emph/eov018.

Cabezón E, Sastre JI, Cruz Fdl. Genetic evidence of a coupling role for the TraG protein family in bacterial conjugation. *Mol Gen Genet* 1997;**254**:400–6. https://doi.org/10.1007/s004380050432.

Carranza G, Menguiano T, Valenzuela-Gómez F *et al.* Monitoring bacterial conjugation by optical microscopy. *Front Microbiol* 2021;**12**:750200. https://doi.org/10.3389/fmicb.2021.750200.

Carraro N, Durand R, Rivard N *et al.* Salmonella genomic island 1 (SGI1) reshapes the mating apparatus of IncC conjugative plasmids to promote self-propagation. *PLoS Genet* 2017;**13**:e1006705. https://doi.org/10.1371/journal.pgen.1006705.

Castañeda-Barba S, Top EM, Stalder T. Plasmids, a molecular cornerstone of antimicrobial resistance in the One Health era. *Nat Rev Micro* 2024;**22**:18–32. https://doi.org/10.1038/s41579-023-00926-x.

Ceccarelli D, Daccord A, René M *et al.* Identification of the origin of transfer (oriT) and a new gene required for mobilization of the SXT/R391 family of integrating conjugative elements. *J Bacteriol* 2008;**190**:5328–38. https://doi.org/10.1128/jb.00150-08.

Collins RF, Frye SA, Balasingham S *et al.* Interaction with type IV pili induces structural changes in the bacterial outer membrane secretin PilQ. *J Biol Chem* 2005;**280**:18923–30. https://doi.org/10.1074/jbc.M411603200.

Coluzzi C, Garcillán-Barcia MP, Cruz Fdl *et al.* Evolution of plasmid mobility: origin and fate of conjugative and nonconjuga-

tive plasmids. *Mol Biol Evol* 2022;**39**:msac115. https://doi.org/10.1093/molbev/msac115.

De Langhe N, Van Dorpe S, Guilbert N *et al.* Mapping bacterial extracellular vesicle research: insights, best practices and knowledge gaps. *Nat Commun* 2024;**15**:9410. https://doi.org/10.1038/s41467-024-53279-1.

Dell'Annunziata F, Folliero V, Giugliano R *et al.* Gene transfer potential of outer membrane vesicles of Gram-negative bacteria. *IJMS* 2021;**22**:5985. https://doi.org/10.3390/ijms22115985.

Dionisio F, Zilhão R, Gama JA. Interactions between plasmids and other mobile genetic elements affect their transmission and persistence. *Plasmid* 2019;**102**:29–36. https://doi.org/10.1016/j.plasmid.2019.01.003.

Fogarty EC, Schechter MS, Lolans K *et al.* A cryptic plasmid is among the most numerous genetic elements in the human gut. *Cell* 2024;**187**:1206–1222.e16. https://doi.org/10.1016/j.cell.2024.01.039.

Fulsundar S, Harms K, Flaten GE *et al.* Gene transfer potential of outer membrane vesicles of *Acinetobacter baylyi* and effects of stress on vesiculation. *Appl Environ Microb* 2014;**80**:3469–83. https://doi.org/10.1128/AEM.04248-13.

Garcillán-Barcia MP,Cuartas-Lanza R, Cuevas A *et al.* Cis-acting relaxases guarantee independent mobilization of MOBQ4 plasmids. *Front Microbiol* 2019;**10**. https://doi.org/10.3389/fmicb.2019.02557.

Garcillán-Barcia MP, de la Cruz F, Rocha EPC. The extended mobility of plasmids. *Nucleic Acids Res* 2025;**53**. https://doi.org/10.1093/nar/gkaf652.

Guerrero-Mandujano A, Hernández-Cortez C, Ibarra JA *et al.* The outer membrane vesicles: secretion system type zero. *Traffic* 2017;**18**:425–32. https://doi.org/10.1111/tra.12488.

Haase J, Lurz R, Grahn AM *et al.* Bacterial conjugation mediated by plasmid RP4: RSF1010 mobilization, donor-specific phage propagation, and pilus production require the same Tra2 core components of a proposed DNA transport complex. *J Bacteriol* 1995;**177**:4779–91. https://doi.org/10.1128/jb.177.16.4779-4791.1995.

Haudiquet M, Sousa JMd, Touchon M *et al.* Selfish, promiscuous and sometimes useful: how mobile genetic elements drive horizontal gene transfer in microbial populations. *Philos Trans R Soc Lond B Biol Sci* 2022;**377**:20210234. https://doi.org/10.1098/rstb.2021.0234.

Hindson BJ, Ness KD, Masquelier DA *et al.* High-throughput droplet digital PCR system for absolute quantitation of DNA copy number. *Anal Chem* 2011;**83**:8604–10. https://doi.org/10.1021/ac202028g.

Johnson TJ, Nolan LK. Plasmid replicon typing. In: Caugant DA (ed.), *Molecular Epidemiology of Microorganisms: Methods and Protocols*. Totowa, NJ: Humana Press, 2009, 27–35. https://doi.org/10.1007/978-1-60327-999-4_3

Johnson JS, Spakowicz DJ, Hong BY *et al.* Evaluation of 16S rRNA gene sequencing for species and strain-level microbiome analysis. *Nat Commun* 2019;**10**:5029. https://doi.org/10.1038/s41467-019-13036-1.

Klümper U, Droumpali A, Dechesne A *et al.* Novel assay to measure the plasmid mobilizing potential of mixed microbial communities. *Front Microbiol* 2014;**5**. https://doi.org/10.3389/fmicb.2014.00730.

Klümper U, Riber L, Dechesne A *et al.* Broad host range plasmids can invade an unexpectedly diverse fraction of a soil bacterial community. *ISME J* 2015;**9**:934–45. https://doi.org/10.1038/ismej.2014.191.

Kulp AJ, Sun B, Ai T *et al.* Genome-wide assessment of outer membrane vesicle production in *Escherichia coli*. *PLoS One* 2015;**10**:e0139200. https://doi.org/10.1371/journal.pone.0139200.

Llosa M, Zunzunegui S, Cruz Fdl. Conjugative coupling proteins interact with cognate and heterologous VirB10-like proteins while exhibiting specificity for cognate relaxosomes. *Proc Natl Acad Sci USA* 2003;**100**:10465–70. https://doi.org/10.1073/pnas.1830264100.

Lorenz MG, Wackernagel W. Bacterial gene transfer by natural genetic transformation in the environment. *Microbiol Rev* 1994;**58**:563–602. https://doi.org/10.1128/mr.58.3.563-602.1994.

Manning AJ, Kuehn MJ. Contribution of bacterial outer membrane vesicles to innate bacterial defense. *BMC Microbiol* 2011;**11**:258. https://doi.org/10.1186/1471-2180-11-258.

McBroom AJ, Johnson AP, Vemulapalli S *et al.* Outer membrane vesicle production by *Escherichia coli* is independent of membrane instability. *J Bacteriol* 2006;**188**:5385–92. https://doi.org/10.1128/jb.00498-06.

Meyer R. Replication and conjugative mobilization of broad host-range IncQ plasmids. *Plasmid* 2009;**62**:57–70. https://doi.org/10.1016/j.plasmid.2009.05.001.

Meyer R, Hinds M, Brasch M. Properties of R1162, a broad-host-range, high-copy-number plasmid. *J Bacteriol* 1982;**150**. https://doi.org/10.1128/jb.150.2.552-562.1982.

Muyzer G, Waal ECd, Uitterlinden AG. Profiling of complex microbial populations by denaturing gradient gel electrophoresis analysis of polymerase chain reaction-amplified genes coding for 16S rRNA. *Appl Environ Microb* 1993;**59**:695–700. https://doi.org/10.1128/aem.59.3.695-700.1993.

Nagakubo T, Nomura N, Toyofuku M. Cracking open bacterial membrane vesicles. *Front Microbiol* 2020;**10**. https://doi.org/10.3389/fmicb.2019.03026.

Nelson KE, Weinel C, Paulsen IT *et al.* Complete genome sequence and comparative analysis of the metabolically versatile Pseudomonas putida KT2440. *Environ Microbiol* 2002;**4**:799–808. https://doi.org/10.1046/j.1462-2920.2002.00366.x.

Norman A, Hansen LH, Sørensen SJ. Conjugative plasmids: vessels of the communal gene pool. *Phil Trans R Soc B* 2009;**364**:2275–89. https://doi.org/10.1098/rstb.2009.0037.

Orench-Rivera N, Kuehn M. Environmentally-controlled bacterial vesicle-mediated export. *Cellular Microbiology* 2016;**18**:1525–36. https://doi.org/10.1111/cmi.12676.

Parker C, Meyer RJ. The R1162 relaxase/primase contains two, type IV transport signals that require the small plasmid protein MobB. *Mol Microbiol* 2007;**66**:252–61. https://doi.org/10.1111/j.1365-2958.2007.05925.x.

Petersen J, Vollmers J, Ringel V *et al.* A marine plasmid hitchhiking vast phylogenetic and geographic distances. *Proc Natl Acad Sci USA* 2019;**116**:20568–73. https://doi.org/10.1073/pnas.1905878116.

Posit Team. *RStudio: integrated Development Environment for R*. Posit Software. PBC, Boston, MA, 2024. http://www.posit.co (13 February 2026, date last accessed).

Rima M, Dakramanji M, El Hayek E *et al.* Unveiling the wonders of bacteria-derived extracellular vesicles: from fundamental func-

tions to beneficial applications. *Heliyon* 2025;**11**:e42509. https://doi.org/10.1016/j.heliyon.2025.e42509.

Roier S, Zingl FG, Cakar F *et al.* Bacterial outer membrane vesicle biogenesis: a new mechanism and its implications. *Microbial Cell* 2016;**3**:257–9. https://doi.org/10.15698/mic2016.06.508.

San Millan A, MacLean RC. Fitness costs of plasmids: a limit to plasmid transmission. *Microbiol Spectr* 2017;**5**. https://doi.org/10.1128/microbiolspec.mtbp-0016-2017

Schwechheimer C, Kuehn MJ. Outer-membrane vesicles from Gram-negative bacteria: biogenesis and functions. *Nat Rev Micro* 2015;**13**:605–19. https://doi.org/10.1038/nrmicro3525.

Segura RL, Águila-Arcos S, Ugarte-Uribe B *et al.* Subcellular location of the coupling protein TrwB and the role of its transmembrane domain. *Biochim Biophys Acta (BBA)—Biomembr* 2014;**1838**:223–30. https://doi.org/10.1016/j.bbamem.2013.08.016.

Smillie C, Garcillán-Barcia MP, Francia MV *et al.* Mobility of plasmids. *Microbiol Mol Biol Rev* 2010;**74**:434–52. https://doi.org/10.1128/mmbr.00020-10.

Takano S, Takenawa S, Naradasu D *et al.* Enrichment of horizontally transferred gene clusters in bacterial extracellular vesicles via non lytic mechanisms. *ISME J* 2025;**19**:wraf193. https://doi.org/10.1093/ismejo/wraf193.

Tamayo-Leiva J, Alcorta J, Sepúlveda F *et al.* Structure and dispersion of the conjugative mobilome in surface ocean bacterioplankton. *ISME Commun* 2024;**4**:ycae059. https://doi.org/10.1093/ismeco/ycae059.

Tato I, Zunzunegui S, Cruz Fdl *et al.* TrwB, the coupling protein involved in DNA transport during bacterial conjugation, is a DNA-dependent ATPase. *Proc Natl Acad Sci USA* 2005;**102**:8156–61. https://doi.org/10.1073/pnas.0503402102.

Thomas CM, Nielsen KM. Mechanisms of, and barriers to, horizontal gene transfer between bacteria. *Nat Rev Micro* 2005;**3**:711–21. https://doi.org/10.1038/nrmicro1234.

Toyofuku M, Nomura N, Eberl L. Types and origins of bacterial membrane vesicles. *Nat Rev Micro* 2019;**17**:13–24. https://doi.org/10.1038/s41579-018-0112-2.

Toyofuku M, Schild S, Kaparakis-Liaskos M *et al.* Composition and functions of bacterial membrane vesicles. *Nat Rev Micro* 2023;**21**:415–30. https://doi.org/10.1038/s41579-023-00875-5.

Tran F, Boedicker JQ. Genetic cargo and bacterial species set the rate of vesicle-mediated horizontal gene transfer. *Sci Rep* 2017;**7**:8813. https://doi.org/10.1038/s41598-017-07447-7.

Tran F, Boedicker JQ. Plasmid characteristics modulate the propensity of gene exchange in bacterial vesicles. *J Bacteriol* 2019:**201**. https://doi.org/10.1128/jb.00430-18

Turnbull L, Toyofuku M, Hynen AL *et al.* Explosive cell lysis as a mechanism for the biogenesis of bacterial membrane vesicles and biofilms. *Nat Commun* 2016;**7**:11220. https://doi.org/10.1038/ncomms11220.

Wen AX, Herman C. Horizontal gene transfer and beyond: the delivery of biological matter by bacterial membrane vesicles to host and bacterial cells. *Curr Opin Microbiol* 2024;**81**:102525. https://doi.org/10.1016/j.mib.2024.102525.

Wickham H. Data Analysis. In: Wickham H (ed.), *Ggplot2: Elegant Graphics for Data Analysis*. Cham: Springer International Publishing, 2016, 189–201. https://doi.org/10.1007/978-3-319-24277-4_9.

Wintersdorff CJHv,PendersJ, Niekerk JMv *et al.* Dissemination of antimicrobial resistance in microbial ecosystems through horizontal gene transfer. *Front Microbiol* 2016;**7**. https://doi.org/10.3389/fmicb.2016.00173.

Yao S, Helinski DR, Toukdarian A. Localization of the naturally occurring plasmid ColE1 at the cell pole. *J Bacteriol* 2007;**189**:1946–53. https://doi.org/10.1128/jb.01451-06.

Zhang X, Ding W, Yang J *et al.* Mechanisms of outer membrane vesicles in bacterial drug resistance: insights and implications. *Biochimie* 2025;**238**:77–90, https://doi.org/10.1016/j.biochi.2025.07.024.

Zhu L, Huang H, Avellán-Llaguno RD *et al.* Diverse functional genes harboured in extracellular vesicles from environmental and human microbiota. *J of Extracellular Vesicle* 2022;**11**:12292. https://doi.org/10.1002/jev2.12292.

Received: 17 July 2026. **Revised:** 21 September 2026. **Accepted:** 27 October 2026

© The Author(s) 2026. Published by Oxford University Press on behalf of FEMS. This is an Open Access article distributed under the terms of the Creative Commons Attribution-NonCommercial License (https://creativecommons.org/licenses/by-nc/4.0/), which permits non-commercial re-use, distribution, and reproduction in any medium, provided the original work is properly cited. For commercial re-use, please contact reprints@oup.com for reprints and translation rights for reprints. All other permissions can be obtained through our RightsLink service via the Permissions link on the article page on our site-for further information please contact journals.permissions@oup.com